

Power-law modeling based on least-squares criteria: consequences for system analysis and simulation

Benito Hernández-Bermejo^a, Víctor Fairén^a, Albert Sorribas^{b,*}

^a *Departamento de Física Matemática y Fluidos, Universidad Nacional de Educación a Distancia. Senda del Rey S/N, 28040 Madrid, Spain*

^b *Departament de Ciències Mèdiques Bàsiques, Universitat de Lleida, Av. Rovira, Roure 44, 25198 Lleida, Spain*

Received 28 September 1999; received in revised form 13 June 2000; accepted 17 July 2000

Abstract

The power-law formalism was initially derived as a Taylor series approximation in logarithmic space for kinetic rate-laws. The resulting models, either as generalized mass action (GMA) or as S-systems models, allow to characterize the target system and to simulate its dynamical behavior in response to external perturbations and parameter changes. This approach has been successfully used as a modeling tool in many applications from cell metabolism to population dynamics. Without leaving the general formalism, we recently proposed to derive the power-law representation in an alternative way that uses least-squares (LS) minimization instead of the traditional derivation based on Taylor series [B. Hernández-Bermejo, V. Fairén, A. Sorribas, *Math. Biosci.* 161 (1999) 83–94]. It was shown that the resulting LS power-law mimics the target rate-law in a wider range of concentration values than the classical power-law, and that the prediction of the steady-state using the LS power-law is closer to the actual steady-state of the target system. However, many implications of this alternative approach remained to be established. We explore some of them in the present work. Firstly, we extend the definition of the LS power-law within a given operating interval in such a way that no preferred operating point is selected. Besides providing an alternative to the classical Taylor power-law, that can be considered a particular case when the operating interval is reduced to a single point, the LS power-law so defined is consistent with the results that can be obtained by fitting experimental data points. Secondly, we show that the LS approach leads to a system description, either as an S-system or a GMA model, in which the systemic properties (such as the steady-state prediction or the log-gains) appear averaged over the corresponding interval when compared with the properties that can be computed from Taylor-derived models in different operating points within the considered operating range. Finally, we also show that the LS description leads to a global, accurate description of the system when it is submitted to external forcing. © 2000 Elsevier Science Inc. All rights reserved.

Keywords: Enzyme kinetics; Metabolism; In situ experiments; S-system; Generalized mass action; Sensitivity analysis

* Corresponding author. Tel.: +34-73 702 403; fax: +34-73 702 426.

E-mail addresses: bhernand@apphys.uned.es (B. Hernández-Bermejo), albert.sorribas@cmb.udl.es (A. Sorribas).

1. Introduction

The power-law approach provides a useful strategy for modeling complex biochemical systems by providing a suitable representation of the underlying rate-laws [2–14]. The traditional recipe within the power-law formalism for approximating any general differentiable target function $v_r(X_1, X_2, \dots, X_{n+m})$, is to use a Taylor series approximation in logarithmic coordinates. This yields

$$v_r \doteq \frac{v_{r0}}{\prod_{j=1}^{n+m} X_{j0}^{f_{rj}}} \prod_{j=1}^{n+m} X_j^{f_{rj}} \equiv \gamma_r \prod_{j=1}^{n+m} X_j^{f_{rj}}. \quad (1)$$

In this power-law representation of the target function v_r , the parameters f_{rj} are known as *kinetic-orders* and have a definite interpretation as a result of the Taylor series approximation of v_r

$$f_{rj} = \left(\frac{\partial v_r}{\partial X_j} \right)_0 \frac{X_{j0}}{v_{r0}}, \quad (2)$$

where the subscript 0 indicates the operating point. The parameter γ_r is known as *rate-constant* and its interpretation is clear from (1). This interpretation of the power-law parameters as local sensitivities is on the basis of many applications of this technique. In particular, it is the starting point for relating the kinetic-orders with experimental measurements through different strategies (see [15–19] for details). Using this approach, a suitable representation of v_r can be derived even in the case that its actual functional form is unknown. This is an important property that allows the use of the power-law formalism as a foundation for modeling complex systems and for discussing their properties and design principles.

Using the power-law formalism for building up a mathematical model of a target system leads to a canonical representation, either a generalized mass action (GMA) model or an S-system model, that greatly facilitates the analysis of the system properties [12–14]. As an illustration, let us consider a kinetic pathway of the form

$$\dot{X}_i = V_i^+(X_1, X_2, \dots, X_{n+m}) - V_i^-(X_1, X_2, \dots, X_{n+m}), \quad (3)$$

where $i = 1, \dots, n$ runs for the dependent variables, m indicates the number of independent variables and the inflows V_i^+ and outflows V_i^- can possibly be decomposed as the sum of other functions describing different contributions to the velocity. The power-law representation (1) allows to build a mathematical model of (3) in the familiar S-system format [8–10,12–14]:

$$\dot{X}_i = \alpha_i \prod_{j=1}^{n+m} X_j^{g_{ij}} - \beta_i \prod_{j=1}^{n+m} X_j^{h_{ij}}, \quad i = 1, \dots, n, \quad (4)$$

where α_i and β_i are called rate constants and g_{ij} and h_{ij} are called kinetic-orders. From this representation, using the notation: $a_{ij} = g_{ij} - h_{ij}$ with $j = 1, \dots, n$ for A_D and $j = (n+1), \dots, (n+m)$ for A_I ; $y_k = \log(X_k)$ with $k = 1, \dots, n$ for Y_I and $k = (n+1), \dots, (n+m)$ for Y_I ; $b_i = \log(\beta_i/\alpha_i)$ for B , it is possible to analytically express the steady-state solution as [8–10,12–14]

$$Y_D = -A_D^{-1} \cdot A_I \cdot Y_I + A_D^{-1} \cdot B. \quad (5)$$

According to (5), the steady-state prediction for any of the dependent variables, Y_D , in these classes of models is a linear function of the independent variables, Y_I , in logarithmic space. This

can be interpreted, in the classical formulation of the power-law formalism, as the first-order approximation in the Taylor series expansion of the actual, often unknown, steady-state solution of the target system around the operating point. Consequently, the solution in (5) is tangent to the actual solution for the considered system and it accurately reflects the behavior of the actual steady-state for sufficiently small deviations around the reference operating point. Despite the apparent limitation of this approach, it has been shown that, in many cases, the steady-state predictions remain accurate over wide ranges of the independent variables [12–14,20].

Although the preceding results can be adequate for many applications, sometimes it may be desirable to give a description of the system over a range which cannot be covered by its approximation at a single operating point. This is the case, for instance, if the system is subjected to sufficiently wide variations of the independent variables. In such cases it is more convenient to think of an operating interval, rather than a single operating point. Then, if the evolution of the system is such that it can move through the whole operating interval, a collection of local, Taylor-based S-systems, each being accurate for a given subinterval of the operating range, will not be suitable in order to provide a unified description of the dynamics over the entire range. At this point, we need a different approach to cover the target range. One possibility is using recasting techniques to exactly represent the target function by means of a power-law [21,22]. Alternatively, we can look for a method that, without leaving the power-law formalism, would lead to a better representation of the observed phenomena within the selected range. Certainly, it might happen that a global description for the considered range, whatever it is, will not be as accurate, at a given point, as the corresponding local S-system description for the subinterval containing that point. However, the advantage of a model of the entire operating interval is obvious – it is the only one that can be helpful if the actual dynamics of the system over the entire range is to be considered.

In a previous work [1], it was shown that a least-squares (LS) minimization provides an alternative way for defining the power-law approximation for rate-laws. In [1], the least-squares approximation was derived by requiring the resulting power-law function to pass through the selected operating point within a considered operating interval. This is a requirement in the Taylor power-law and it seemed appropriate to derive the least-squares power-law in the same fashion. However, the idea of fitting a least-squares power-law within a range can be further elaborated if we relax that condition. This new formulation is more consistent with the results that can be obtained by fitting experimental data and opens new perspectives in modeling the target system. In this paper, we shall explore the implications of this new strategy focusing on the steady-state characterization and on the prediction of the system's dynamic response. Furthermore, we shall briefly discuss the fitting of a power-law to experimental data as a method for obtaining a suitable model for the intact system.

2. Least-squares power-law modeling

2.1. Why a least-squares power-law? Deriving a power-law representation from experimental data

The power-law strategy is very useful when the underlying rate-law is unknown. In such a case, it is possible to derive a mathematical representation provided we know the variables that modify the target rate-law. For instance, a model of the thyroid hormone metabolism may consider the

regulation of the TSH release V_{TSH}^- within the anterior pituitary (see [23] for details). This process is regulated by T_3 and T_4 and has the internal TSH_I concentration as a substrate. On the other hand, the hormone TRH produced by the hypothalamus can stimulate this process. We can represent this process as

$$V_{\text{TSH}}^- = V_{\text{TSH}}^-(T_3, T_4, \text{TSH}_I, \text{TRH}). \quad (6)$$

At the biological level, (6) is an aggregated process that includes different individual reactions, probably including enzymatic and transport systems. At the modeling level, it may suffice to consider the overall process and all the variables that influence it. Consequently, because this is a particular conceptualization of this process, no kinetic characterization could be found in the literature. This makes it difficult, a priori, to select a specific kinetic function to represent this process in a mathematical model of thyroid metabolism. The power-law representation can be easily written and is a valid alternative in this case

$$V_{\text{TSH}}^- = \gamma_{\text{TSH}} T_3^{f_{T_3}} T_4^{f_{T_4}} \text{TSH}_I^{f_{\text{TSH}_I}} \text{TRH}^{f_{\text{TRH}}}. \quad (7)$$

Although the actual function V_{TSH}^- is unknown, the rationale behind the Taylor power-law allows one to write (7) from scratch using qualitative information. The theory behind this representation predicts that this function will accurately represent the actual function around the reference operating point. Parameter estimation can now proceed in several ways. Qualitative considerations can be used to suggest some tentative values. For instance, if we want to consider that a process is first-order for a given variable, we can immediately take a kinetic-order of one. On the other hand, partial observations on the intact system can provide some clues on the parameters. For instance, if a 10% increase in T_3 would lead to a 25% inhibition in TSH release, then we can adjust f_{T_3} to reflect this observation (see [15,16,23] for an account of methods).

Alternatively, one could experimentally measure the target rate at different values of the involved variables and fit a power-law function to the data points. To simplify the exposition, we shall consider a single variable process

$$v = v(X) = \gamma X^f. \quad (8)$$

Measurement of v for different values of X would lead to a set of data points that can be used to obtain the parameters in the power-law showed in (8). The least-squares criteria can be written as

$$\sum_{i=1}^s (v_i - \gamma X_i^f)^2 \rightarrow \text{MINIMUM}. \quad (9)$$

As an example, in Fig. 1 we show simulated data and the resulting power-law fit in different situations. If we use this strategy, no operating point is selected and the overall range of variation of X is taken as the region of approximation of the target process. Accordingly, the power-laws obtained for each case do not correspond to a Taylor power-law since they are not tangent to the velocity curves. Furthermore, as it results from the data shown in Fig. 1, the obtained LS power-law functions provide an overall accurate description of the observed velocities within the considered range. It is worth noting that the LS fit produces a single power-law for a given set of experimental data. This would be different if we were to follow the Taylor strategy that would produce a different power-law for each operating point selected. Of course, the different LS power-laws obtained for each set of data are an estimation of the corresponding LS power-law repre-

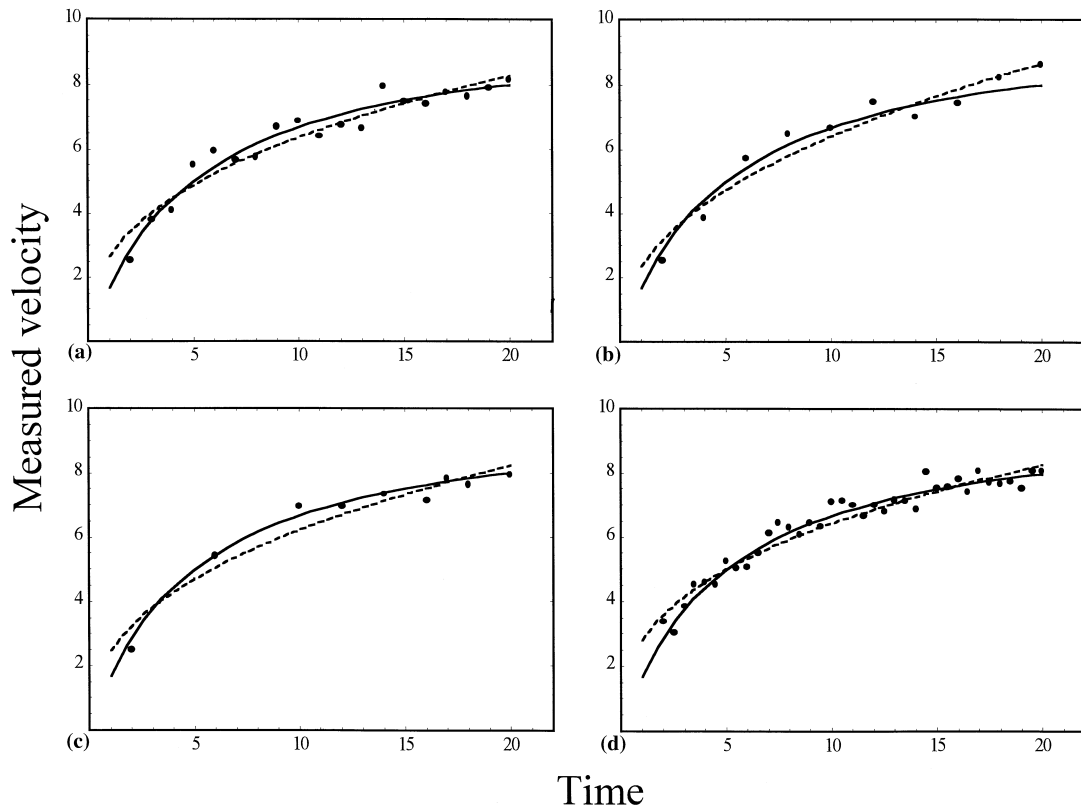


Fig. 1. Fitting of a power-law function to experimental data. Data points are simulated from the same kinetic equation with a random variation and different sample points for the independent variable. The dotted line indicates the LS power-law that fits the data points. The continuous line indicates the underlying kinetic equation from which data points are simulated. The LS power-law parameters obtained for each data set are: (a) $\alpha = 2.65, f = 0.38$; (b) $\alpha = 2.35, f = 0.44$; (c) $\alpha = 2.46, f = 0.40$; (d) $\alpha = 2.80, f = 0.36$.

sensation of the underlying function within the operating range of X . We shall elaborate on this idea and explore its implications for characterizing the target system.

2.2. Least-squares power-law of a given function

In a previous paper [1], we proposed an alternative strategy for obtaining a power-law representation of a target function $v_r(X_1, \dots, X_n)$. In this formulation of the least-squares criterion, minimization was constrained within the operating interval $\Omega = [L_1, U_1] \times [L_2, U_2] \times \dots \times [L_n, U_n]$, so that for a given operating point $(X_{10}, \dots, X_{n0}) \in \Omega$ we have $v_r(X_{10}, \dots, X_{n0}) = \gamma_r \prod_{i=1}^n X_{i0}^{f_i}$. This condition can be relaxed to obtain a least-squares representation that is optimal within an overall range in which no preferential operational point is considered. Instead of the traditional Taylor-like algorithm, which is essentially of local nature (the approximating power-law is determined by the behavior of v in a single point, i.e. the operating point), we will presently consider the power-law approximation of v_r which is optimum in the sense of LS, i.e. such that the following integral achieves a minimum:

$$\left(\int_{\Omega} \left[v(X_1, \dots, X_n) - \gamma_r \prod_{j=1}^n X_j^{f_{rj}} \right]^2 dX_1 \cdots dX_n \right)^{1/2} \rightarrow \text{MINIMUM.} \quad (10)$$

Thus, the problem amounts to determining the set of LS kinetic orders f_{rj} and the LS rate constant γ_r , which do not coincide in general with those in (2). Moreover, as it has been shown in the previous section, this approach is in natural correspondence with the data analysis of experimentally measured flux (see below).

It is important to stress that minimization of (10) will produce a unique power-law representation for the whole range (see Appendix A). As said, this minimization requires the target function $v_r(X_1, \dots, X_n)$ to be known. Fitting experimental data will produce an estimation of this optimal power-law, the quality of which will depend on the experimental design. Although this issue would require a deeper discussion and the analysis of actual data, we shall include a simulation example to show the possibilities of this approach. In the following, we shall first focus on the results obtainable from the original functions through minimization of (10). Then we shall discuss an example of deriving a power-law model through the LS approach using data from the whole system.

3. Steady-state characterization and system's dynamics using a least-squares derived power-law model

3.1. Alternative S-system representations using Taylor and least-squares strategies

As was illustrated for some simple cases in our previous paper [1], the least-squares approach can ameliorate substantially the quality of the representation of a given velocity – for example, the LS fitting can account in a more realistic way for the saturation property of the velocity. This is a consequence of the fact that in an LS approximation, all points of the operating interval in which function v is to be approximated are equally weighted, i.e. they are equally relevant. This gives an important degree of flexibility to the LS method, since we can choose the most convenient operating interval for each situation – a degree of flexibility not present in a Taylor-based scheme. Once we have established the appropriateness of the least-squares approach, it is necessary to explore in more detail the consequences of this new perspective.

Firstly, as the obtained power-law is formally similar to the Taylor power-law, in both cases we will obtain an S-system model, or the corresponding GMA alternative model, for the target system. Which is the interpretation of the steady-state characterization if we use the LS strategy? Secondly, how do the Taylor and the LS power-law models relate when we compare the dynamic responses? For the sake of clarity, it is simpler to answer these questions by means of a detailed example.

The first issue to explore concerns the interpretation of the steady-state characterization of a given S-system. In the case of a Taylor based S-system, logarithmic gains and sensitivities have a clear interpretation that relates to the Taylor series approximation of the actual solution. In practice, in this approach logarithmic gains and parameter sensitivities are global sensitivities in the sense of sensitivity theory. How must we interpret a logarithmic gain when the S-system is

derived from LS? The question is relevant since, for a given operating interval, we can have infinite Taylor approximations but only one LS approximation. Each of the Taylor models characterizes the system’s response in the considered operating point, while the LS model produces a unique characterization for the whole interval. Which is the interpretation of the LS characterization? To clarify this point, we shall use a reference model defined in terms of kinetic equations. This model will be used to produce a reference steady-state that can be used to compare the Taylor and LS strategies. In a real application, the underlying equations would be generally unknown and the analysis carried out on experimental measurements.

The reference system is shown in Fig. 2. In this system, X_1 and X_2 are internal metabolites, and X_3 is an external metabolite whose concentration can be experimentally controlled. We shall assume that the system is initially given as

$$\dot{X}_1 = v_1(X_2, X_3) - v_2(X_1), \tag{11}$$

$$\dot{X}_2 = v_2(X_1) - v_3(X_2). \tag{12}$$

We may consider, for example, the following typical situation, which will define our reference system for comparing the Taylor and LS approaches:

$$v_1 = \frac{10X_3}{3(1 + 0.5X_2) + X_3}, \quad v_2 = \frac{24X_1^2}{7(20 + X_1^2)}, \quad v_3 = \frac{260X_2}{21(10 + X_2)}. \tag{13}$$

Let us first concentrate on the form of the steady-state dependence of X_1 and X_2 in terms of X_3 (Fig. 3). Suppose we take $2 \leq X_3 \leq 7$ as our operating interval. Within this interval the steady value of X_2 behaves almost linearly as a function of X_3 . In that case, any of the possible Taylor S-systems would provide a good fit for practical purposes. On the contrary, this is not the case for the X_1 versus X_3 curve. The non-linearity of the X_1 steady-state curve would make difficult to capture it by a single Taylor S-system. This makes X_1 especially suitable in order to critically compare the two different power-law approximations – LS and Taylor.

The notable non-linearity in the X_1 steady-state dependence on X_3 suggests that local, Taylor-based S-systems derived for Eqs. (11)–(13) might not be the best possible option in order to give a unified description of the original system over the entire operating interval. We shall see that this is the case independently of the choice of the operating point within the interval – even though some operating points will certainly lead to better predictions than the rest. To check these statements, we can first approximate the velocities (13) in system corresponding to Eqs. (11) and (12) according to the standard Taylor approach corresponding to Eqs. (1) and (2). This cannot be done in a unique way, since we first need to fix an operating point. A representative sample of operating points is given by the extremes and the middle point of the interval, i.e. X_{30} equal to 2.0, 4.5, and 7.0. With these values, the resulting steady-states corresponding to model Eqs. (11)–(13) are

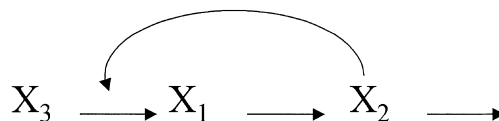


Fig. 2. Metabolic scheme of system (11)–(13).

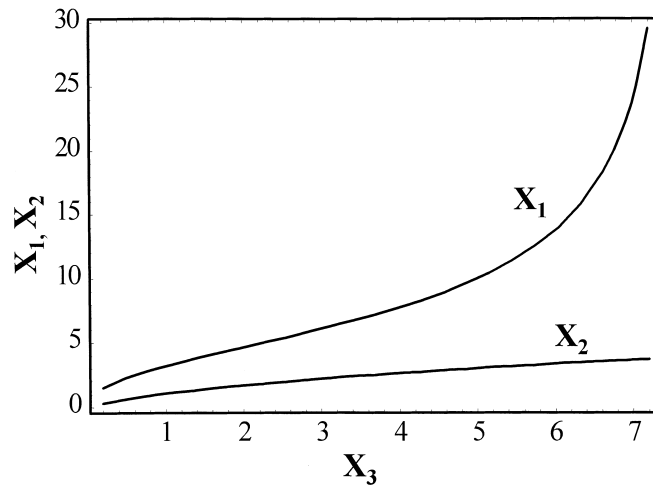


Fig. 3. Steady-state value of X_1 and X_2 , versus X_3 for system (11)–(13).

$$(X_{10}, X_{20}, X_{30}) = \{P_1 = (4.658, 1.684, 2);$$

$$P_2 = (8.767, 2.816, 4.5); \quad P_3 = (23.892, 3.653, 7)\}. \quad (14)$$

The standard procedure to derive the corresponding Taylor power-laws yields the following three S-systems:

$$\text{Model I: } \dot{X}_1 = 1.228X_2^{-0.376}X_3^{0.822} - 0.408X_1^{0.959}, \quad (15)$$

$$\dot{X}_2 = 0.408X_1^{0.959} - 1.142X_2^{0.856}, \quad (16)$$

at P_1

$$\text{Model II: } \dot{X}_1 = 1.414X_2^{-0.423}X_3^{0.728} - 1.110X_1^{0.413}, \quad (17)$$

$$\dot{X}_2 = 1.110X_1^{0.413} - 1.213X_2^{0.780}, \quad (18)$$

at P_2 and

$$\text{Model III: } \dot{X}_1 = 1.578X_2^{-0.432}X_3^{0.669} - 2.672X_1^{0.068}, \quad (19)$$

$$\dot{X}_2 = 2.672X_1^{0.068} - 1.282X_2^{0.732}, \quad (20)$$

at P_3 .

Let us now derive the LS alternative. We thus approximate each of the velocities in (13) by their optimal LS power-laws. For the sake of illustration, one of the resulting LS approximate velocities is shown in Fig. 4. Notice how the LS power-law is not tangent to the exact velocity at any point.

After approximating the velocities we are led to a resulting model that differs from any of the previous Taylor-like S-systems, namely

$$\text{Model IV: } \dot{X}_1 = 1.347X_2^{-0.384}X_3^{0.723} - 1.446X_1^{0.277}, \quad (21)$$

$$\dot{X}_2 = 1.446X_1^{0.277} - 1.195X_2^{0.791}. \quad (22)$$

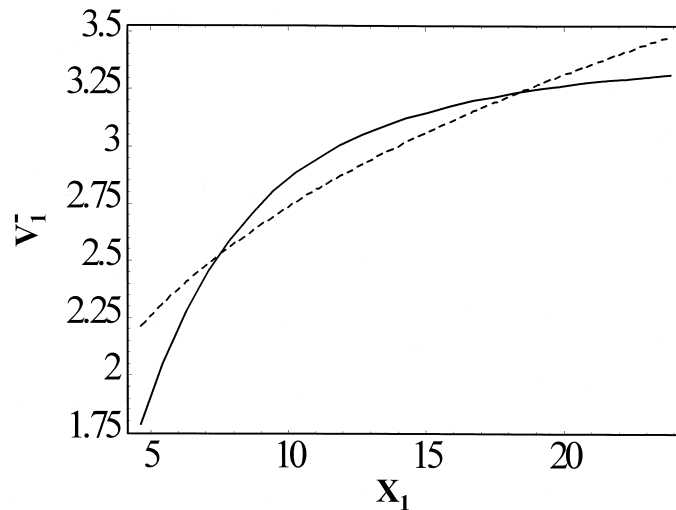


Fig. 4. LS approximation of the velocity $v_2(X_1) = V_1^-$ within the operating range. The LS approximation is indicated as a dashed line.

We shall now compare all these four S-systems from two points of view: the steady-state characterization and the model's response to changes in the external variable.

3.2. Steady-state characterization

As indicated in (5), the steady-state solution of an S-system is linear in log–log space. Accordingly, this solution is a power-law in normal space and corresponds to an approximation to the actual steady-state of the target system. As an illustration, we can compare graphs of the steady state prediction of X_1 versus X_3 . This is done in Fig. 5 for the Taylor S-systems derived at the operating points P_1 (Model I), P_2 (Model II), and P_3 (Model III). These predictions are compared with the actual solution from (13). In each case, it is worth recalling that each one of the three S-system predictions is tangent to the actual solution.

We can now look at the steady-state prediction given by the S-system obtained from the least-squares power-law approximation (Model IV). As is shown in Fig. 6, the estimated curve is not tangent to the exact solution at any point. Consequently, the LS solution does not correspond to any of the possible Taylor S-systems. The LS result is, as expected, an average estimation over the whole interval. As we said before, a local, Taylor-based prediction will be probably more accurate in the neighborhood of the chosen operating point. However, in the LS representation there is not a privileged operating point but a whole interval of points for which we look for the best representation. Accordingly, the LS solution will be, on the average, more accurate than any of the possible Taylor based solutions over the whole interval.

It is worth mentioning also that the LS steady-state prediction does not correspond mathematically to the least-squares power-law fitting of the actual solution. It can be seen, however, that typically both will be close in relative terms (we elaborate on this in Appendix B) and the LS estimation of the steady state can be considered, from a practical point of view, as a good estimation of the power-law least-squares approximation of the actual solution.

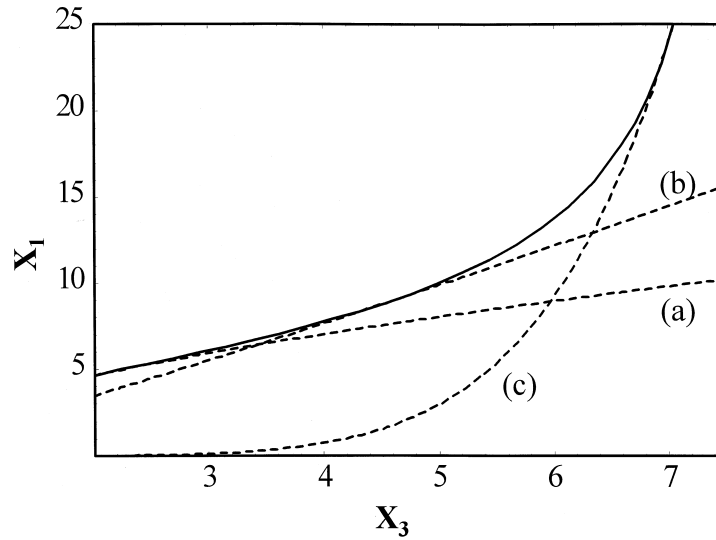


Fig. 5. Comparative steady-state predictions for X_1 versus X_3 for system (11)–(13). The exact solution (solid line) is shown together with the Taylor power-law approximations (dotted lines) obtained when the operating point is chosen at (a) $X_{30} = 2$, (b) $X_{30} = 4.5$ and (c) $X_{30} = 7$.

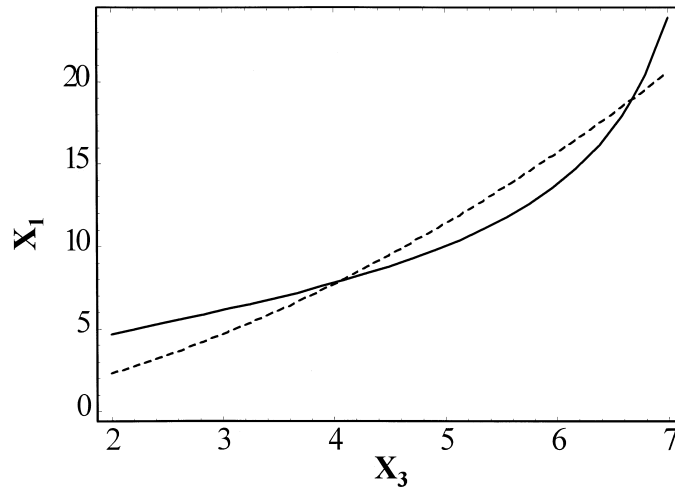


Fig. 6. Least-squares steady-state predictions for X_1 versus X_3 for system (11)–(13). The exact solution (solid line) is shown together with the least-squares power-law approximation (dotted line) obtained for the operating interval $2 \leq X_3 \leq 7$.

3.3. Sensitivity analysis

The LS strategy leads to an S-system model from which the usual steady-state characterization can be derived. For instance, in an S-system model, logarithmic-gains quantify the change in a dependent variable as a response to a change in an independent variable. Logarithmic-gains can be obtained from matrix L

Table 1

Different logarithmic gains of the steady-state prediction of X_1 and X_2 in terms of X_3 over the operating interval, for both the Taylor and the LS methods

X_3	X_1 Log-gain	X_2 Log-gain
2	0.59532	0.66718
3	0.74081	0.63375
4	0.97011	0.61206
5	1.37615	0.59633
6	2.28756	0.58413
7	6.21267	0.57424
Mean (6 points)	2.03044	0.61128
Mean (10 points)	1.81002	0.61004
Mean (50 points)	1.64690	0.60907
Mean (100 points)	1.62823	0.60895
Mean (300 points)	1.61605	0.60887
LS S-system	1.75788	0.61495

$$L = -A_D^{-1} \cdot A_1. \quad (23)$$

Formally, in the Taylor approach a logarithmic-gain is the slope of the steady-state solution predicted by (5) in logarithmic space. Which is the meaning of the logarithmic-gains derived from the LS representations? Both the Taylor and the LS predictions of the steady-state are straight lines in logarithmic plane (Eq. (5).) The Taylor-based method produces one different approximating line per operating point, thus giving a different estimation of the gain for every point in the operating interval. On the contrary, the LS method leads to a unique approximation for the whole interval, thus giving a unique, averaged value for the gain over the operating range (Table 1).

3.4. Dynamical aspects

By definition, it is to be expected that the LS approach will be especially useful in those cases in which the dynamics deviates from the range of validity of the Taylor approach. This may happen, for instance, if the system is externally driven. We shall assume a forcing of the system by some function $X_3(t)$. We can thus find the time evolution of $X_1(t)$ and $X_2(t)$ for the exact system (Eqs. (11)–(13)), and compare it with the estimations provided by both the Taylor and the LS methods. Due to the fact that the sharpest differences between the LS and the Taylor approximations can be observed on X_1 , we shall choose this variable in order to clearly monitorize the differences between both approaches. Regarding the Taylor algorithm, we shall work on three operating points: The center of the operating interval ($X_{30} = 4.5$) and both extremes $X_{30} = 2$ and $X_{30} = 7$. The first one is probably one of the most balanced choices for the Taylor method, while the extremes of the interval can result in advantageous choices if the system is forced into the extremes of the operating range.

For the time variation of X_3 we shall consider the case of a chaotic dependence. For this, we shall use Rössler's equations, rewritten in GMA form and with a convenient choice of parameters [22]

$$\dot{z}_1 = z_2 - z_3, \tag{24}$$

$$\dot{z}_2 = 0.36z_2 - z_1, \tag{25}$$

$$\dot{z}_3 = z_1z_3 - 22.5z_3 - 49.6z_1 + 1117.8. \tag{26}$$

We take as initial conditions $z_1(0) = 18, z_2(0) = 47$ and $z_3(0) = 50$. To obtain the desired chaotic signal in X_3 we use the transformation

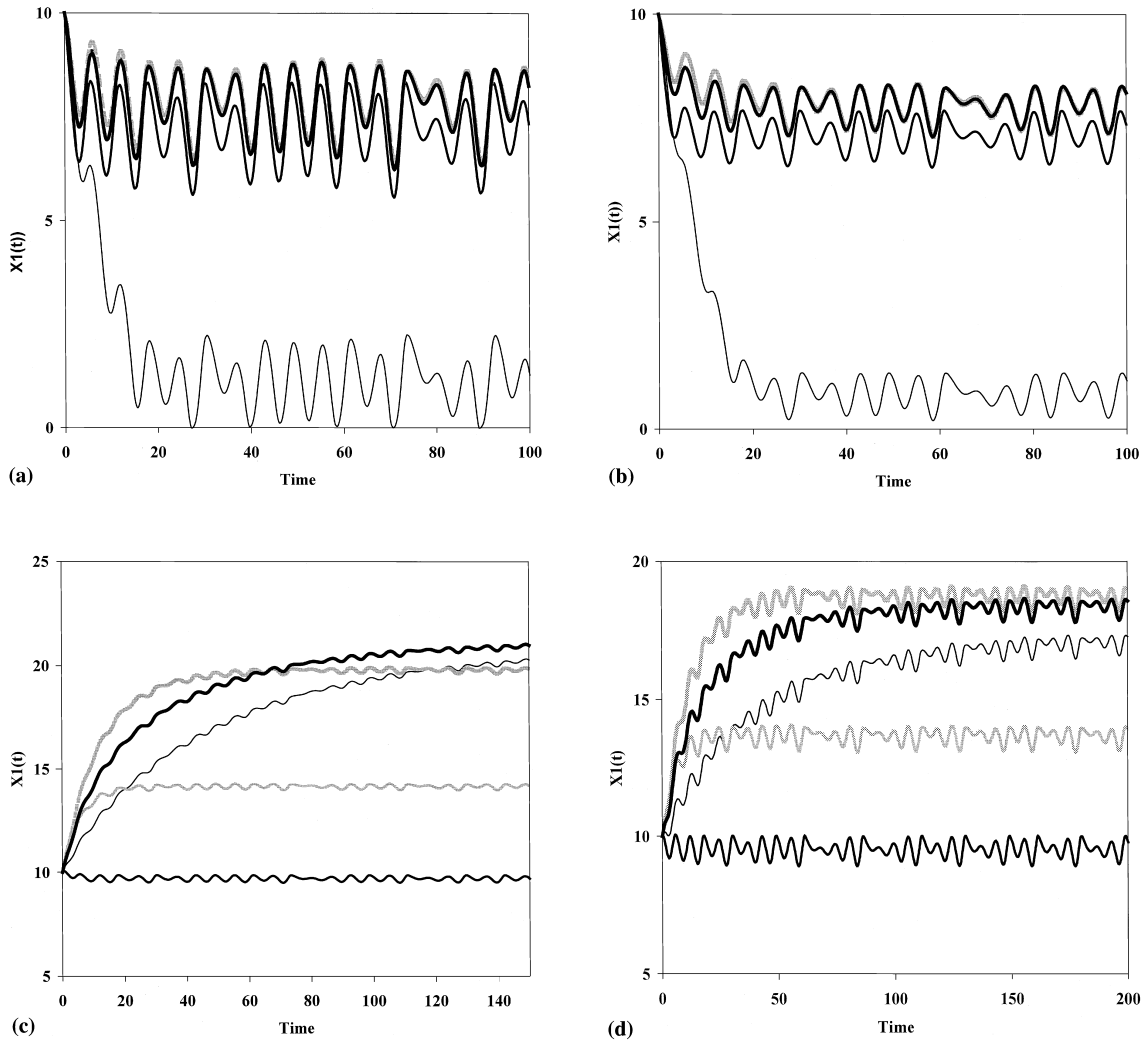


Fig. 7. Time evolution of X_1 with chaotic forcing in X_3 . The exact solution (thickest black line) is displayed together with the LS solution (thickest grey line) and the three Taylor solutions (medium thickness black line for P_1 , thin grey line for P_2 , and thin black line for P_3): (a) $\alpha = \beta = 2$ (X_3 oscillates over the entire operating range); (b) $\alpha = 4, \beta = 3$ (X_3 oscillates between 3 and 5); (c) $\alpha = 12, \beta = 6.5$ (X_3 oscillates around 6.8); (d) $\alpha = 4, \beta = 5.6$ (X_3 oscillates between 5.5 and 8). In all cases the initial conditions are $X_1(0) = 10$ and $X_2(0) = 3$. In (a) and (b) the LS and P_2 solutions are almost indistinguishable from the exact solution.

$$X_3(t) = \frac{z_1(t) - 14}{\alpha} + \beta, \tag{27}$$

where we can set α and β in order to fix the average value and the amplitude of the forcing. Several comparisons are displayed in Fig. 7. In all cases, α and β are chosen in such a way that the oscillation of X_3 is bounded within different regions of the operating interval.

Generally speaking, we can say that both the Taylor and the LS methods tend to reproduce with fair accuracy the pattern of oscillations of X_1 . However, in many cases the averaging nature of the LS solution leads to a closer estimation of the time evolution than most Taylor-based predictions – sometimes closer than any of the considered Taylor-based predictions. As expected, one of the Taylor systems may give in some specific cases a better prediction than the LS approximation, but the LS is clearly the best one if we consider the whole interval, thus providing a compact description of the actual system over the operating range in just one single model.

4. Fitting a least-squares power-law model to data obtained on an intact system

Power-law models provide a valuable modeling tool for a given system. Their fundamental advantage, as we have discussed in a previous section, is that the mathematical representation for the different rates is provided by a rather simple mathematical function. Despite this simplicity, the final model is adequate for studying system’s properties and dynamic responses within the surroundings of an operating point.

In this paper, we have discussed the advantages of deriving this representation from a new perspective: the least-squares power-law representation of the target rate-law. We have shown that the resulting representation is adequate and how it is related to the usual Taylor-derived power-law. Now, we shall turn to the application of the LS strategy to the analysis of data obtained on the intact system. The point is to show how to obtain a power-law model if data on the actual system were available. We shall consider data corresponding to steady-state measurements of flux and concentrations for different values of the external variables. In such a case, the system is explored in a range of values of these variables, and the election of a single operating point may be not the most convenient possibility.

As a reference pathway for discussing the fit of a power-law LS model, we shall use the hypothetical pathway shown in Fig. 8. To simulate this system, a set of enzyme rate-laws is selected (see Appendix C). From the reference model, a Taylor–GMA model is derived at the operating point: $X_7 = 3, X_8 = 5$. This model is

$$\begin{aligned} \dot{X}_1 &= 0.100952X_7^{1.87508}X_5^{-0.902837} - 1.8706X_1^{1.75015}, \\ \dot{X}_2 &= 1.8706X_1^{1.75015} - 0.036679X_2^{1.87508}X_6^{-0.916405}, \\ \dot{X}_3 &= 0.122197X_8^{1.52854}X_5^{-0.735981} - 1.25069X_3^{1.52854}, \\ \dot{X}_4 &= 1.25069X_3^{1.52854} - 0.0838928X_4^{1.52854}X_6^{-0.747041}, \\ \dot{X}_5 &= 0.036679X_2^{1.87508}X_6^{-0.916405} + 0.0838928X_4^{1.52854}X_6^{-0.747041} - 1.28821X_5^{1.27869}, \\ \dot{X}_6 &= 1.28821X_5^{1.27869} - 1.28821X_6^{1.27869}. \end{aligned} \tag{28}$$

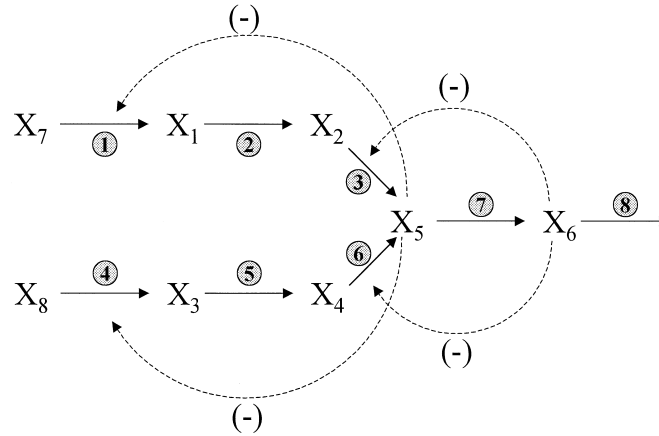


Fig. 8. Reference metabolic pathway. X_7 and X_8 are external variables that can be experimentally fixed. Dotted lines indicate regulatory signals. The circled numbers correspond to enzyme reactions (see text and Appendix C for details).

Simulated experiments are performed at different values of the independent variables by computing the resulting steady-state flux and concentrations. In each case, random error is introduced as indicated in Appendix C. The LS power-law model is fitted for each velocity using the obtained data points (Fig. 9). The resulting model is

$$\begin{aligned}
 \dot{X}_1 &= 0.129274 X_7^{1.69816} X_5^{-0.883239} - 1.5858 X_1^{1.29586}, \\
 \dot{X}_2 &= 1.5858 X_1^{1.29586} - 0.0508275 X_2^{1.66596} X_6^{-0.765177}, \\
 \dot{X}_3 &= 0.141724 X_8^{1.42718} X_5^{-0.717182} - 1.22311 X_3^{1.44826}, \\
 \dot{X}_4 &= 1.22311 X_3^{1.44826} - 0.0924435 X_4^{1.44753} X_6^{-0.686011}, \\
 \dot{X}_5 &= 0.0508275 X_2^{1.66596} X_6^{-0.765177} + 0.0924435 X_4^{1.44753} X_6^{-0.686011} - 1.53047 X_5^{0.852397}, \\
 \dot{X}_6 &= 1.53047 X_5^{0.852397} - 1.52499 X_6^{0.858319}.
 \end{aligned} \tag{29}$$

Although both approaches yield similar models, the LS strategy produces a better approximation to the actual one (Fig. 9). The LS minimization results in a power-law representation that may be more adequate than the Taylor representation at a given operating point (Fig. 9(a)–(b)). It is worth noting that the relevant range of variation of the dependent variables may be far more restricted than the potential range for the same variable studied *in vitro*. In the case of a velocity that is a function of several variables, as it is the case of v_1 or v_4 in the reference system, the resulting data are an approximated sample of the corresponding surface within the operating range considered. For instance, as a consequence of the system constraints, X_5 changes only between 1 and 3 in the set of simulated experiments using the X_7 and X_8 set of values indicated in Appendix C (Fig. 9(c)–(d)). Then, the resulting rate-law should account for the measured velocities and needs not consider the full range of potential values. In such case, the power-law is a good alternative for building a realistic model for these velocities.

The performance of the LS power-law can be better appreciated in dynamic simulations. In Fig. 10 we simulate the system dynamics to different perturbations. In each case, we consider a

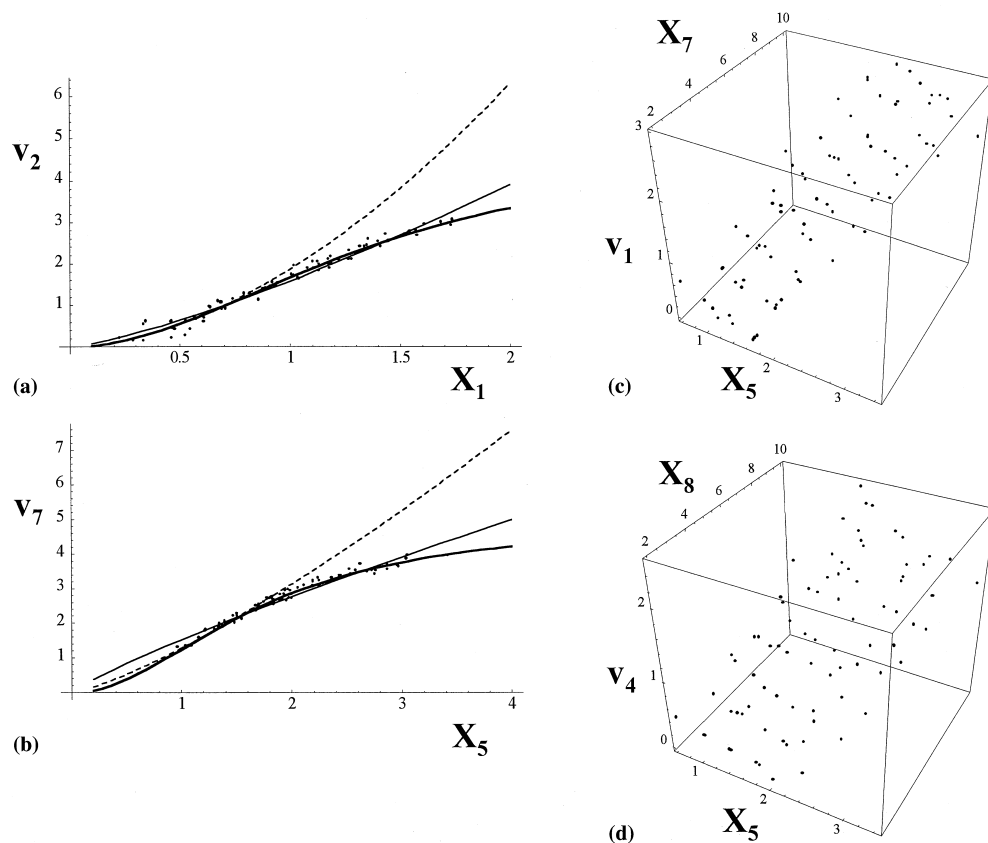


Fig. 9. LS power-law fitting to data. Simulated experiments are used as data for fitting the corresponding LS power-law representation. In (a) and (b) dots indicates the measured velocity for a given value of the considered variable. The actual rate-law is depicted in black. A continuous grey line indicates the LS power-law fitting to those data. The corresponding Taylor representation at the operating point is indicated by a dotted line. In (c) and (d) the experimental points for v_1 and v_4 are indicated. For clarity, the surfaces corresponding to the different approaches are not shown. They correspond to Eqs. (28), (29) and (C.1).

momentary increment in X_6 . In the first experiment, X_7 and X_8 are changed from the original values. In the second experiment, they are maintained at the reference values. It can be clearly appreciated that the LS–GMA model provides a better representation of the underlying dynamics in both cases. Although one can imagine other experiments in which the Taylor approach can be also a good representation, these results show the potential utility of the LS approach. Furthermore, as the experimental data consist in a series of concentration and rate measurements, it seems far more adequate to use the LS approach.

5. Final comments

We have seen that the LS method is a natural strategy in order to derive the representation of a metabolic pathway in the framework of the power-law formalism over sufficiently wide operating

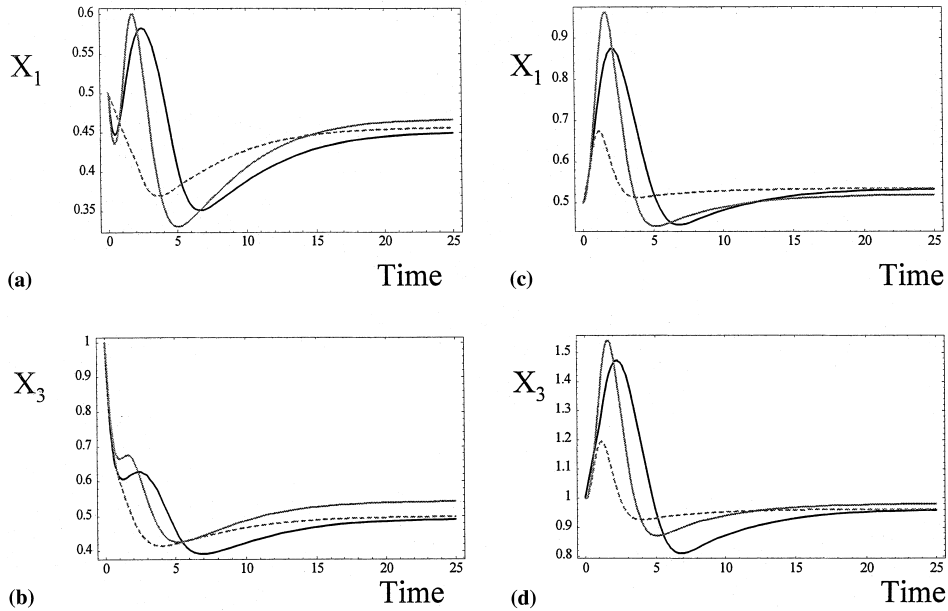


Fig. 10. Dynamic simulations. In these experiments, the predictions from the GMA model derived from the LS power-law equations are compared to the reference system and to the Taylor-GMA. The reference system is indicated by a black line. The LS-GMA is indicated by a continuous grey line. The Taylor-GMA is indicated by a dotted grey line. For each case, the initial conditions for $\{X_1, X_2, \dots, X_8\}$ are: (a) and (b) $\{0.5, 5, 1, 6, 1.3, 20, 2, 2\}$; (c) and (d) $\{0.5, 5, 1, 6, 1.3, 20, 3, 5\}$.

intervals. This methodology does not represent a contradiction with the traditional Taylor-based procedure, of which it is a generalization: as was shown in [1], the LS and the Taylor approximations do coincide in the limit of small operating intervals or, more precisely, in the limit in which the operating interval reduces to a single point.

From a practical point of view, this means that the LS method may be the most convenient choice in almost every case, and not only in those in which the system fluctuates. In those cases in which the system does not deviate substantially from a given point, the LS result will be very similar to the Taylor one. However, there is a conceptual difference between both attitudes: A Taylor-based methodology assumes a somehow static picture of the evolution of the system, since such evolution is considered as taking place on a single point, and every deviation from such point is, essentially, also a deviation from the basic modeling hypotheses underlying the method. On the contrary, in the LS approach it is assumed that real systems are subjected to variations and fluctuations of very different nature, and therefore the modeling strategy must be adapted from the very beginning to contemplate such phenomena as a part of the problem. This leads, as we have seen, to models that describe reality in a global, averaged way. These models have also proven to be appropriate for obtaining the accurate predictions within the considered operating range.

Finally, it is worth recalling that the LS reformulation of the power-law formalism is quite natural from the experimental point of view. When our input is not a differential model, but a set of experimental points, the problem is how to develop a modeling strategy leading to the dif-

ferential description. Clearly, the concept of derivative, which is the basis of the Taylor-based power-law, is of limited application in this context. On the contrary, a LS regression of the data appears more appropriate. This is, among other reasons, why we suggest that the LS approach might provide the basis for deriving the power-law representation, specially in the case where experimental data are the starting point. A preliminary analysis of the problem shows that such approach is adequate. In a forthcoming paper we shall discuss in detail the advantages of the LS strategy when the system’s model is to be derived from experimental measurements of the actual velocities and concentrations in situ.

Acknowledgements

This work has been supported by the DGICYT of Spain (grants PB94-0390 and PM96-0099). A.S. acknowledges a grant from La Paeria, Lleida (X0148), and a grant from FIS (00/0235).

Appendix A. Uniqueness of the optimal LS power-law approximation

Consider a velocity function $v(X_1, \dots, X_{n+m})$ defined on a domain Ω in which we seek the LS minimization to a power-law of the form

$$v(X_1, \dots, X_{n+m}) \doteq \gamma \prod_{j=1}^{n+m} X_j^{g_j}. \tag{A.1}$$

Assume that the global minimum is *not* unique, i.e. there exist at least two different power-laws

$$p_i(X_1, \dots, X_{n+m}) = \gamma_i \prod_{j=1}^{n+m} X_j^{g_{ij}}, \quad i = 1, 2, \tag{A.2}$$

such that the minimization integral takes the same minimum value for both

$$\left(\int_{\Omega} [v - p_i]^2 dX_1 \cdots dX_{n+m} \right)^{1/2} = \mu \rightarrow \text{MINIMUM}, \quad i = 1, 2. \tag{A.3}$$

If we square and subtract both expressions, this implies in particular that

$$\int_{\Omega} [p_1^2 - p_2^2 + 2v(p_2 - p_1)] dX_1 \cdots dX_{n+m} = 0. \tag{A.4}$$

Let us define $\varepsilon(X_1, \dots, X_{n+m}) = p_1 - p_2$ in Ω . Then, after some simple algebra integral (A.4) can be written as

$$\int_{\Omega} \varepsilon[p_1 + p_2 - 2v] dX_1 \cdots dX_{n+m} = 0. \tag{A.5}$$

Now, both p_1 and p_2 are approximations to v in Ω , so the difference $p_1 + p_2 - 2v$ will be typically small in absolute value when compared to v . Also, $p_1 + p_2 - 2v$ will be a vanishing function on a subset of Ω of zero measure. However, $p_1 + p_2 - 2v$ is not zero in general (apart from the trivial

case in which v itself is a power-law, in which the uniqueness problem is straightforward). Therefore, the term $p_1 + p_2 - 2v$ cannot generically account for the cancellation of integral (A.5). This means that the only possibility is that $\varepsilon(X_1, \dots, X_{n+m}) = 0$, i.e. that $p_1 = p_2$, actually. Therefore we have reached a contradiction and the LS minimum is unique.

Appendix B. Least-squares properties of the steady-state prediction

As indicated in Section 3.2, here we shall give some estimations regarding the closeness between the LS steady-state prediction and the power-law LS fit of the exact steady-state function. We shall consider for the sake of simplicity the case corresponding to one independent and one dependent variable. There is no lack of generality in this, since the argument can be straightforwardly generalized to a higher number of variables.

Consider a steady-state equation of the form

$$v_1(X_I, X_D) = v_2(X_I, X_D). \tag{B.1}$$

Assuming that the hypotheses of the implicit function theorem are verified (which will be the case in practice) then there exists a unique function $\varphi(\xi)$ such that

$$X_D = \varphi(X_I). \tag{B.2}$$

Of course, $\varphi(\xi)$ will be unknown in most practical situations, but for what follows we only need to know that it exists. Then, there exists an optimal LS power-law approach to φ in the corresponding domain

$$X_D \doteq \gamma X_I^g \tag{B.3}$$

For simplicity, we shall call this function $p(X_I)$, i.e. $p(X_I) = \gamma X_I^g$. We thus have that

$$I(\gamma, g) = \left(\int_{\Omega} (\varphi(X_I) - \gamma X_I^g)^2 dX_I \right)^{1/2} \tag{B.4}$$

is minimum.

It is possible to find an approximation of (B.3) as follows. We first approximate v_1 and v_2 by means of their LS power-laws

$$v_1(X_I, X_D) \doteq \mu_1 X_I^{\rho_{11}} X_D^{\rho_{12}}, \tag{B.5}$$

$$v_2(X_I, X_D) \doteq \mu_2 X_I^{\rho_{21}} X_D^{\rho_{22}}. \tag{B.6}$$

Then, after equating the right-hand sides of (B.5) and (B.6) we immediately arrive to an approximate solution of Eq. (B.1)

$$X_D \doteq \tilde{\gamma} X_I^{\tilde{g}}. \tag{B.7}$$

This is the LS approximation for the steady-state. We shall again set $\tilde{p}(X_I) = \tilde{\gamma} X_I^{\tilde{g}}$. The problem is to know to what extent the following integral:

$$I'(\tilde{\gamma}, \tilde{g}) = \left(\int_{\Omega} (\varphi(X_I) - \tilde{\gamma} X_I^{\tilde{g}})^2 dX_I \right)^{1/2} \tag{B.8}$$

is close to the minimum (B.4). In order to establish the closeness between I' and I , we should first note that

$$I' = I\sqrt{1 + \frac{I_C}{I^2}}, \tag{B.9}$$

where

$$I_C = \int_{\Omega} (p - \tilde{p})(2\varphi - p - \tilde{p}) dX_I \tag{B.10}$$

Eqs. (B.9) and (B.10) can be obtained easily from (B.8). Now notice that typically we have $|p - \tilde{p}| \ll |\varphi - p|$ for most points of the operating interval, since both p and \tilde{p} have the same power-law form and \tilde{p} is an approximation of p . On the contrary, φ is not a power-law in general, so the difference $|\varphi - p|$ will be much larger than $|p - \tilde{p}|$, in spite of the fact that p is the best LS power-law fit of φ . For example, in the case of system (11)–(13) we have (Fig. 11) that p and \tilde{p} are exceedingly close, and their difference is certainly smaller in absolute value than $\varphi - p$ for most points of the interval.

Consequently, after examining the integrands of I_C and I^2 we conclude that

$$I_C \simeq \int_{\Omega} 2(p - \tilde{p})(\varphi - p) dX_I \ll I^2 \tag{B.11}$$

and therefore

$$\frac{I_C}{I^2} \ll 1. \tag{B.12}$$

According to (B.9), this implies that I' is close to the minimum I in relative terms, as we expected. For example, in the case of model Eqs. (11)–(13) we easily find $I' \simeq 1.13I$, thus being a good estimation of the true minimum.

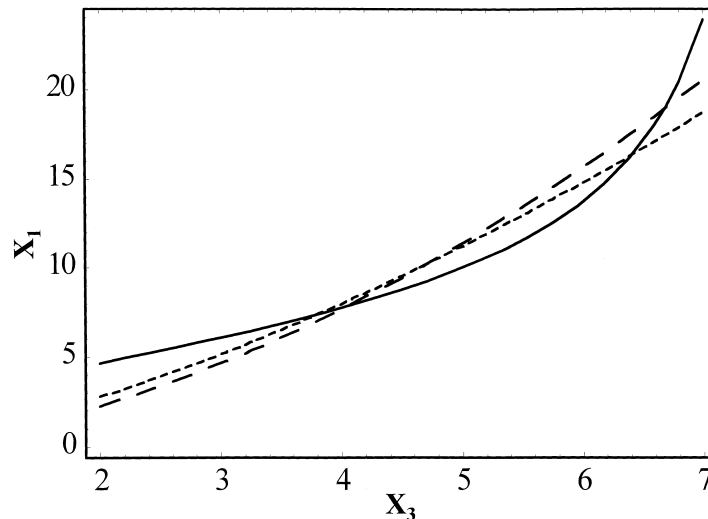


Fig. 11. Plot of the exact steady-state solution $\varphi(X_3)$ (continuous line), its LS power-law fit $p(X_3)$ (- - -) and the approximation obtained in Section 3.2 $\tilde{p}(X_3)$ (- · -) for variable X_1 of system (11)–(13).

Appendix C. Reference model for Section 4

The model depicted in Fig. 9 has been used to simulate steady-state measurements. For each of the pathway reactions, a rate-law has been selected

$$\begin{aligned}
 v_1 &= \frac{10X_7^2}{5(1 + X_5/0.05) + X_7^2}, \\
 v_2 &= \frac{10X_2^2}{2 + X_1^2}, \\
 v_3 &= \frac{10X_2^2}{9(1 + X_6/0.03) + X_2^2}, \\
 v_4 &= \frac{5X_8^2}{3(1 + X_5/0.05) + X_8^2}, \\
 v_5 &= \frac{5X_3^2}{3 + X_3^2}, \\
 v_6 &= \frac{5X_4^2}{3(1 + X_6/0.03) + X_4^2}.
 \end{aligned} \tag{C.1}$$

Using (C.1), the reference model is

$$\begin{aligned}
 \dot{X}_1 &= v_1 - v_2, \\
 \dot{X}_2 &= v_2 - v_3, \\
 \dot{X}_3 &= v_4 - v_5, \\
 \dot{X}_4 &= v_5 - v_6, \\
 \dot{X}_5 &= v_3 + v_6 - v_7, \\
 \dot{X}_6 &= v_7 - v_8.
 \end{aligned} \tag{C.2}$$

The steady-state values for the dependent variables X_1 – X_6 are computed from (C.2) for different values of the independent variables X_7 and X_8 . The resulting values are perturbed by adding statistical noise resulting in a 10% error on the unperturbed values (normally distributed with 0 mean). Once the perturbed concentrations are obtained, the corresponding rates are computed using (C.1). The resulting velocities are also perturbed to simulate a 10% experimental error.

The simulated experiment discussed in Section 4 is generated using a grid of values of X_7 and X_8 . In both cases, the values are: 2, 3, 4, ..., 10. The resulting steady-state values for fluxes and concentrations are used as data for the LS fit of the corresponding power-laws. The fitted model is indicated in (29). The Taylor model is computed at the operating point $X_7 = 3$ and $X_8 = 5$. The resulting equations are indicated in (28).

In all cases, results are obtained by using *Mathematica*. Dynamic simulations are performed using the **NDSolve** routine in *Mathematica*.

References

- [1] B. Hernández-Bermejo, V. Fairén, A. Sorribas, Power-law modeling based on least-squares minimization criteria, *Math. Biosci.* 161 (1999) 83.
- [2] R. Curto, A. Sorribas, M. Cascante, Comparative characterization of the fermentation pathway of *Saccharomyces cerevisiae* using biochemical systems theory and metabolic control analysis: model definition and nomenclature, *Math. Biosci.* 130 (1995) 25.
- [3] F. Shiraishi, M.A. Savageau, The tricarboxylic acid cycle in *dictyostelium discoideum*. Formulation of the alternative kinetic representations, *J. Biol. Chem.* 267 (1992) 22912.
- [4] F. Shiraishi, M.A. Savageau, The tricarboxylic acid cycle in *dictyostelium discoideum* II. Evaluation of model consistency and robustness, *J. Biol. Chem.* 267 (1992) 22919.
- [5] F. Shiraishi, M.A. Savageau, The tricarboxylic acid cycle in *dictyostelium discoideum*. III Analysis of steady state and dynamic behavior, *J. Biol. Chem.* 267 (1992) 22926.
- [6] F. Shiraishi, M.A. Savageau, The tricarboxylic acid cycle in *dictyostelium discoideum* IV. Resolution of discrepancies between alternative methods of analysis, *J. Biol. Chem.* 267 (1992) 22934.
- [7] F. Shiraishi, M.A. Savageau, The tricarboxylic acid cycle in *dictyostelium discoideum*. Systemic effects of including protein turnover in the current model, *J. Biol. Chem.* 268 (1993) 16917.
- [8] M.A. Savageau, Biochemical systems analysis: I. Some mathematical properties of the rate law for the component enzymatic reactions, *J. Theoret. Biol.* 25 (1969) 365 1969.
- [9] M.A. Savageau, Biochemical systems analysis II. Steady state solutions for an n-pool system using a power-law approximation, *J. Theoret. Biol.* 25 (1969) 370.
- [10] M.A. Savageau, The behaviour of intact biochemical control systems, *Curr. Tops. Cell. Reg.* 6 (1972) 63.
- [11] A. Sorribas, R. Curto, M. Cascante, Comparative characterization of the fermentation pathway of *Saccharomyces cerevisiae* using biochemical systems theory and metabolic control analysis: model validation and dynamic behavior, *Math. Biosci.* 130 (1995) 71.
- [12] A. Sorribas, M.A. Savageau, A comparison of variant theories of intact biochemical systems. I. Enzyme-enzyme interactions and biochemical systems theory, *Math. Biosci.* 94 (1989) 161.
- [13] A. Sorribas, M.A. Savageau, A comparison of variant theories of intact biochemical systems. II. Flux-oriented and metabolic control theories, *Math. Biosci.* 94 (1989) 195.
- [14] A. Sorribas, M.A. Savageau, Strategies for representing metabolic pathways within biochemical systems theory: reversible pathways, *Math. Biosci.* 94 (1989) 239.
- [15] R. Curto, E.O. Voit, A. Sorribas, M. Cascante, Validation and steady-state analysis of a power-law model of purine metabolism in man, *Bio-chem. J.* 324 (1997) 761.
- [16] R. Curto, E.O. Voit, A. Sorribas, M. Cascante, Mathematical models of purine metabolism in man, *Math. Biosci.* 151 (1998) 1 1998.
- [17] A. Sorribas, M. Cascante, Structure identifiability in metabolic pathways: parameter estimation in models based on the power-law formalism, *Biochem. J.* 298 (1994) 303.
- [18] A. Sorribas, B. Lozano, V. Fairén, Deriving chemical and biochemical model networks from experimental measurements, *Rec. Res. Develop. Phys. Chem.* 2 (1998) 553.
- [19] A. Sorribas, S. Samitier, E.I. Canela, M. Cascante, Metabolic pathway characterization from transient response data obtained in situ: parameter estimation in S-system models, *J. Theor. Biol.* 162 (1993) 81.
- [20] E.O. Voit, M.A. Savageau, Accuracy of alternative representations for integrated biochemical systems, *Biochemistry* 26 (1987) 6869.
- [21] M.A. Savageau, E.O. Voit, Recasting non-linear differential equations as S-systems: a canonical non-linear form, *Math. Biosci.* 87 (1987) 83.
- [22] E.O. Voit, S-system modeling of complex systems with chaotic input, *Environmetrics* 4 (1993) 153.
- [23] A. Sorribas, A. Gonzalez, The power-law formalism as a tool for modeling hormonal systems, *J. Theoret. Med.* 2 (1999) 19.